Proceedings Paper:

Papananias, M. orcid.org/0000-0001-7121-9681, McLeay, T., Mahfouf, M. et al. (1 more author) (2019) An intelligent metrology informatics system based on neural networks for multistage manufacturing processes. In: Procedia CIRP. 17th CIRP Conference on Modelling of Machining Operations, 13-14 Jun 2019, Sheffield, UK. Elsevier , pp. 444-449.

https://doi.org/10.1016/j.procir.2019.04.148

Available online at www.sciencedirect.com

ScienceDirect

Procedia CIRP 82 (2019) 444–449

www.elsevier.com/locate/procedia

17th CIRP Conference on Modelling of Machining Operations

An Intelligent Metrology Informatics System based on Neural Networks for Multistage Manufacturing Processes

Moschos Papananias[a]*, Thomas E McLeay[b], Mahdi Mahfouf[a], Visakan Kadirkamanathan[a]

[a]*Department of Automatic Control and Systems Engineering, The University of Sheffield, Mappin Street, Sheffield S1 3JD, UK*
[b]*Advanced Manufacturing Research Centre with Boeing, The University of Sheffield, Advanced Manufacturing Park, Wallis Way, Catcliffe, Rotherham S60 5TZ, UK*

* Corresponding author. *E-mail address:* m.papananias@sheffield.ac.uk

Abstract

The ability to gather manufacturing data from various workstations has been explored for several decades and the advances in sensory and data acquisition techniques have led to the increasing availability of high-dimensional data. This paper presents an intelligent metrology informatics system to extract useful information from Multistage Manufacturing Process (MMP) data and predict part quality characteristics such as true position and circularity using neural networks. The input data include the tempering temperature, material conditions, force and vibration while the output data include comparative coordinate measurements. The effectiveness of the proposed method is demonstrated using experimental data from a MMP.

Peer-review under responsibility of the scientific committee of The 17th CIRP Conference on Modelling of Machining Operations

Keywords: Multistage Manufacturing; Intelligent/Smart Manufacturing; Manufacturing Informatics; Artificial Neural Networks

1. Introduction

Manufacturing is the process of altering the geometry and properties of a given starting material to produce parts. Metal manufacturing processes usually involve multiple operations such as forming, machining, inspection, assembly and testing to produce a high-quality part or product that performs according to its design specifications. Forming is an important step in manufacturing metallic products to obtain the desired shape and dimensions of the workpiece through mechanical deformation. In addition, once the desired geometry of the workpiece is obtained, it is often necessary to modify the microstructure and mechanical properties of the workpiece, without changing its geometry, using heat treatment techniques. Machining typically includes a series of metal-removing operations to achieve parts with the desired shape, dimensions and surface finish. However, there are many factors, such as cutting parameters, tool wear, cutting forces, vibration, geometric errors, human errors, and environmental effects, that affect the machining process and thus the quality of machined parts [1, 2]. In addition, in multistage manufacturing, where each product goes through multiple processing stages, part quality is also affected by the accumulated errors transmitted from previous processing stages. Therefore, the final part variation is subject to the accumulation of variations from all operations [3].

To ensure product quality and process safety, each operation in a manufacturing system is often monitored using various sensors and software systems [4, 5]. For example, in machining, key process performance indicators such as force, vibration, temperature and Acoustic Emission (AE) data can be obtained during part production. Therefore, manufacturing data belong to the typical family of big data characterized by high volume, velocity, variety and veracity [6, 7].

Statistical Process Control (SPC) is a necessary process to detect early abnormal operating conditions during the

2212-8271 © 2019 The Authors. Published by Elsevier B.V.
Peer-review under responsibility of the scientific committee of The 17th CIRP Conference on Modelling of Machining Operations
10.1016/j.procir.2019.04.148

manufacturing process and diagnose their sources. A major advantage of SPC over post-process inspection is that compensating adjustments can be made in the manufacturing process as the product is manufactured in order to reduce variability and scrap levels. A review of the development of Statistical Process Monitoring (SPM) technology can be found in [7]. Traditional SPC is based on univariate statistical methods. One of the main disadvantages of this approach is the complexity in monitoring the control charts as the number of variables increases. Control charts are SPC tools that have been traditionally used in the manufacturing industry to monitor variability. Multivariate Statistical Process Control (MSPC) approaches treat the variables simultaneously and often use latent variable methods to exploit the correlation of measured variables and deal with missing and noisy data [7, 8]. In order to cope with dimensionality reduction, multivariate statistical techniques such as Principal Component Analysis (PCA) are generally used. PCA projects the information in the process variables into a low-dimensional space defined by a few latent variables. Ferrer [9] illustrated the practical benefits of PCA-based MSPC over conventional SPC in an autobody assembly process.

The fourth industrial revolution (Industry 4.0) moves from automated to autonomous intelligent/smart manufacturing. Therefore, efficient big data and predictive analytics tools are required to extract useful information from a manufacturing process and improve manufacturing efficiency for a wide range of manufacturing conditions using Artificial Intelligence (AI) models. Artificial Neural Networks (ANNs) are one of the most commonly used AI tools in SPC applications due to their ability to learn and model complex and nonlinear relationships [10-12].

Over the years, many research efforts have been made to develop intelligent monitoring systems for machining processes using sensor measurements of the process and machine learning models. Most publications are focused on tool wear and machined surface roughness monitoring systems. Özel and Karpat [13] developed models based on feedforward neural networks to predict both surface roughness and tool flank wear in finish hard turning using workpiece hardness, cutting speed, feed rate, axial cutting length and the mean values of cutting forces. Salgado et al. [14] presented a method based on Least Squares Support Vector Machines (LS-SVMs) to predict surface roughness for turning processes using cutting parameters, tool geometry parameters and features extracted from vibration signals by utilizing Singular Spectrum Analysis (SSA). Huang [15] developed an intelligent neural-fuzzy in-process surface roughness monitoring system for an end milling operation using cutting parameters (spindle speed, feed rate and depth of cut) and cutting force signals (the average resultant peak force and the absolute average force).

This paper presents a new system for intelligent manufacturing that learns from in-process metrology data and predicts the final condition of a product. Compared to most previous research focusing on monitoring the machining processes to identify the finish-machined part condition, this system, based on neural networks, is novel given it uses data from multiple different processes to predict the end product quality. A case study is presented where metrology data comes available as each product goes through the steps of heat treatment and machining. The measured variables used as model inputs include the tempering temperature, material conditions, force and vibration. Comparative coordinate measurements are used as output variables to train the models. The performance of the proposed method is demonstrated by predicting the true position and circularity of a circular feature.

The remainder of the paper is organized as follows. Section 2 describes ANNs. Section 3 presents the experimental work performed to produce the parts and obtain the multistage manufacturing data required to validate the proposed method. Section 4 develops the intelligent metrology informatics system based on ANNs to predict the accuracy of the manufactured parts from the measured variables obtained during production. Finally, concluding remarks are given in Section 5.

2. Artificial neural networks

ANNs are human brain-inspired computing systems intended to replicate the human learning process. The most popular neural networks are considered to be the Multi-Layer Perceptron (MLP) networks. An MLP network is a feedforward neural network model consisting of one input layer, one or more hidden layers, and one output layer. Each layer includes one or more nodes. Apart from the input nodes, each node is an artificial neuron. The first model of an artificial neuron was proposed by McCulloch and Pitts [16]. Fig. 1 shows an architectural graph of an MLP network consisting of a number of inputs, one hidden layer with a number of hidden neuros, and one output. Each node in one layer connects (with a certain weight) to every node in the following layer. Each node in the hidden and output layer (artificial neurons) includes: i) a summation unit, which computes a weighted sum over its inputs and adds a bias or threshold term to the sum, and, ii) a nonlinear activation function that is differentiable [17]. However, linear output layer activations are also common [18]. The output of a neuron can be described by:

$$y = f\left(\sum_{i=1}^{n} w_i x_i + b\right) \tag{1}$$

where $f(\cdot)$ is a nonlinear activation function, w_i denotes the synaptic weight coefficient associated with the i-th neuron input, x_i, and b is the bias input.

The MLP network is a supervised network because a desired output is required for learning. A critical step in developing a neural network model involves the selection of the number of neurons in the hidden layer since in most cases a single hidden layer is sufficient. The number of hidden neurons can be determined easily by trial and error. The number of inputs and outputs of the network is determined by the dimensions of the input and output data. The supervised learning technique utilized by an MLP network for training is a particular Back-Propagation (BP) learning algorithm. The BP is an optimization procedure based on gradient descent that adjusts the network's weights in order to minimise the system error computed by the difference between the network output and the desired output.

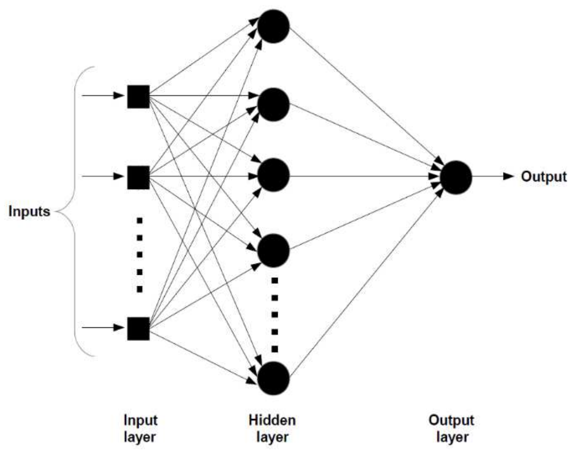

Fig. 1. Architectural graph of an MLP network with one hidden layer and one output.

In this work, two different MATLAB network training functions are used to train the predictive models: i) the Variable Learning Rate Back-Propagation (VLRBP) that updates weight and bias values according to gradient descent momentum and an adaptive learning rate, and, ii) the Conjugate Gradient with Powell/Beale restarts (CGB) that updates weight and bias values according to the conjugate gradient BP with Powell-Beale restarts.

The data required to train the MLP network are the P pattern pairs $\{(\boldsymbol{x}^{(p)}, \boldsymbol{d}^{(p)})\}_{p=1}^{P}$, where $\boldsymbol{x}^{(p)} = [x_1^{(p)}, \dots, x_n^{(p)}]^{\mathrm{T}}$ is the input vector for the p-th pattern and $\boldsymbol{d}^{(p)} = [d_1^{(p)}, \dots, d_m^{(p)}]^{\mathrm{T}}$ is the desired or target vector for the p-th pattern. The Mean Squared Error (MSE) is given by:

$$\begin{aligned} J &= \frac{1}{P}\sum_{p=1}^{P}\left\|\boldsymbol{d}^{(p)} - \boldsymbol{y}^{(p)}\right\|^2 \\ &= \frac{1}{P}\sum_{p=1}^{P}\sum_{i=1}^{m}\left[d_i^{(p)} - y_i^{(p)}\right]^2 \end{aligned} \tag{2}$$

where $\boldsymbol{y}^{(p)} = [y_1^{(p)}, \dots, y_m^{(p)}]^{\mathrm{T}}$ is the output vector for the p-th pattern. Although the method employed in this work uses MLP networks, Elman networks are also developed for comparison with other types of neural networks. Elman networks use positive feedback from the hidden layer to construct some form of memory in the network.

3. Experimental work

This section describes the experimental work performed to produce the parts and obtain metrology data from heat treatment, machining and dimensional inspection. Fig. 2 shows the Computer-Aided-Design (CAD) model of the part. Experimental work was performed using a VECSTAR furnace, a DMG MORI NVX 5080 3-axis machine and a Renishaw Equator 300 Extended Height System, supplied with the SP25 3-axis analogue scanning probe. The material (steel EN24) was heat treated before machining (see Fig. 3). In particular, the material blocks were heated up to 845°C and then quenched in oil for hardening. After hardening, the material blocks were tempered at different temperatures, including 450°C, 550°C and 650°C, to obtain workpieces with different mechanical properties such as material surface hardness. High temperature thermocouples were placed in the furnace to measure temperature gradient and temperature variation during hardening and tempering. Surface hardness measurements were performed on the heat treated blocks using a Rockwell device.

For machining, a full factorial design with four factors at two levels and one center point each was conducted. The factors considered were: material surface hardness, feed rate, spindle speed, and datum error (when the part is flipped around the Y axis for the machining of the second orientation). All the cutting tools used for the machining operations were inspected for wear using a Leica microscope after machining each workpiece. The tool wear was measured on each flute. Each cutting tool was used until it reached a given flank wear width to reduce the influence of tool wear on product variation and measured variables. Coolant was used for all the machining operations. During machining, cutting force data were obtained at 10 kHz using a Kistler dynamometer (9255B), located between the vice holding the workpiece and the machine table, and DynoWare software (see Fig. 4). The dynamometer contains four sensors. The system was configured to output: the sum combination of force signal in the X direction from the first and second sensor; the sum combination of force signal in the X direction from the third and fourth sensor; the sum combination of force signal in the Y direction from the first and fourth sensor; the sum combination of force signal in the Y direction from the second and third sensor; a single force signal in the Z direction from each sensor; and the sum combination of force signals for each direction from all the sensors. In addition, vibration data were obtained at 10 kHz using an accelerometer placed on the spindle and NI LabVIEW SignalExpress software.

The product quality characteristics of interest in this work are the true position and circularity of the large circular feature (see Fig. 2), which were evaluated using the Equator gauge in scanning mode under workshop conditions. The Equator is a Coordinate Measuring System (CMS) operating in comparator mode. Comparative coordinate measurement benefits from the fact that constant systematic effects associated with the measurement system cancel out through the principle of mastering [19-23]. This system provides two main comparison methods: the “Golden Compare” method and the “Coordinate Measuring Machine (CMM) Compare” method. The Golden Compare method requires a reference master part to calibrate the comparator system and assumes that the master part is produced to drawing nominals. Therefore, any deviation of the master part from drawing nominals will be included in the measurements. The most accurate method of using an Equator gauge is the CMM Compare. This method does not require a reference master part to calibrate the comparator system. However, it requires to calibrate a production part, produced close to drawing nominals, on an accurate CMS such as a CMM in order to generate a calibration file for the comparator system.

The calibration file is read by the comparator system during mastering to enable the individual points of a master dataset to be compared with that of test datasets.

The CMM Compare method was employed to calibrate the comparator system. The stylus used was a typical 30 mm long stylus with tungsten carbide stem and a 2 mm diameter ruby ball. The calibration file, required for this Compare method, was generated using a Mitutoyo CMM with a Renishaw REVO RSP3 3D scanning probe (see Fig. 5). The CMM Compare procedure consists of the following steps:

a) Obtain a master part from the production parts.
b) Generate the required part program on the Equator.
c) Edit the part program on the CMM. The part program at this stage should include the commands COMPARE/ON, CAL and COMPARE/OFF.
d) Measure the master part on the CMM to produce a calibration file for the Equator.
e) Transfer the calibration file to the Equator and edit the part program on the Equator to add the commands COMPARE/ON, CAL and COMPARE/OFF.
f) Place the master part on the Equator and run the part program in master mode to produce a master file with reference to the calibration file.
g) Run the part program using the master part in measure mode (verification step).
h) Remove the master part and replace with the production parts to be measured.

CMM accuracy is dependent upon the ambient thermal environment in which it operates because thermal effects degrade CMM accuracy. Therefore, the production of the calibration file required for CMM Compare was performed using a CMM located in a temperature controlled room. According to manufacturer's instructions, it is required to generate more point data from the CMM for CMM Compare using scanning measurements. The required minimum ratio of points measured on the CMM is ten for every single point measured on the Equator. Also, good measurement practice to maintain accuracy on the CMM is to reduce the part program speeds, accelerations and scan velocity according to the CMM's specification. It is worth mentioning that this inspection approach requires repeatable part fixturing because the comparison process involves a point-to-point comparison between the master part data and the test part data. The same fixturing arrangement was used for both the CMM and the Equator gauge. Fig. 6 shows the experimental setup on Equator gauge.

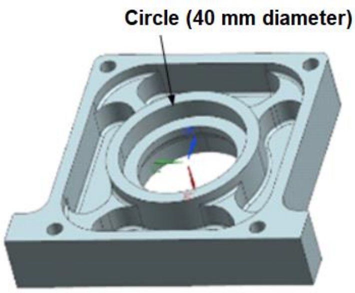

Fig. 2. CAD model of the part.

Fig. 3. Heat treatment.

Fig. 4. Machining.

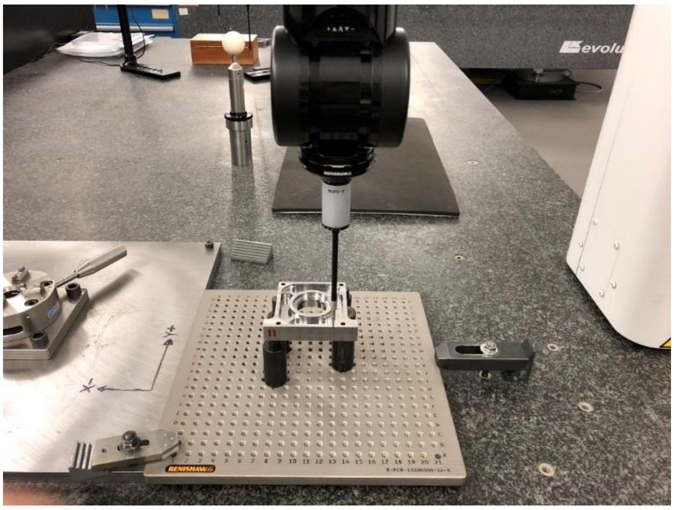

Fig. 5. CMM measurement.

Note that eighteen parts were produced in total; seventeen parts were produced to complete the experimental design (sixteen parts for the base design and one part for the center point) and train and test the predictive models and one part was produced in order to be used as a master part in comparator measurement.

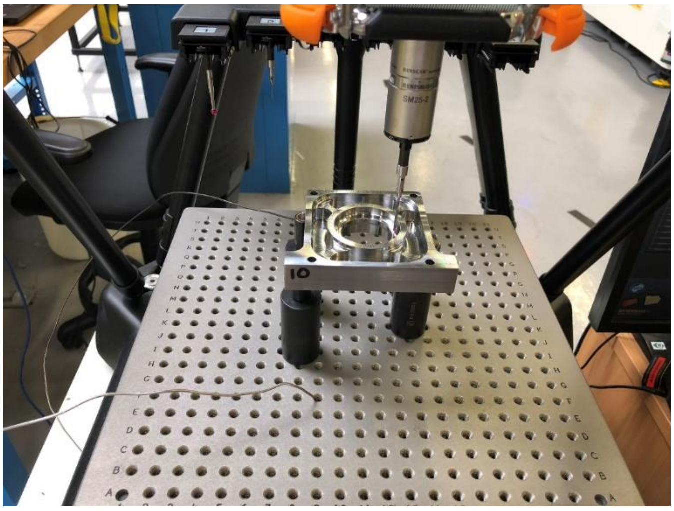

Fig. 6. Comparative coordinate measurement.

4. Metrology informatics system development

To predict the end product quality, an MLP network with eight inputs, one hidden layer consisting of ten neurons, and one output was developed. Tan-sigmoid transfer functions were used for both the hidden and the output layers to provide the nonlinear characteristic to the network. The first three inputs to the MLP network are the Root Mean Square (RMS) values of the sum combination of force signal in the X, Y and Z direction, respectively, from all the four sensors of the dynamometer. The next three inputs to the network are the RMS values of vibration signal in the X, Y and Z direction, respectively. The seventh input is a coded vector corresponding to the surface hardness of the material. The eighth input is the maximum tempering temperature obtained from the five thermocouples during the heat treatment process of the material blocks. The output is the vector of measurand of interest (true position and circularity). To study the linear dependence of the measured data, the correlation coefficients of the network inputs and the desired outputs for the training dataset are shown in Table 1. The correlation between two random variables x and d can be defined in terms of the covariance of the two variables and the product of the standard deviations of the two variables:

$$\rho = \frac{cov(x,d)}{\sigma_x \sigma_d}, \quad -1 \leq \rho \leq 1 \tag{3}$$

Table 1. Correlation coefficients for true position and circularity for the training dataset.

	Network inputs	ρ for true position	ρ for circularity
1	RMS-F_X	0.5119	0.3786
2	RMS-F_Y	0.6134	0.3717
3	RMS-F_Z	0.5080	0.5834
4	RMS-V_X	0.0843	0.4092
5	RMS-V_Y	-0.0334	0.4441
6	RMS-V_Z	-0.1106	0.4084
7	Surface hardness	0.7472	0.3452
8	Tempering temperature	-0.4139	-0.0066

The results in Table 1 indicate the degree of linear dependence between the network inputs and the desired outputs. If the variables are independent, then $\rho = 0$, and the closer the coefficient ρ is to either 1 or -1, the stronger the correlation between the variables.

Data from the manufacture of nine parts were used for training and data from the manufacture of eight parts were used for testing. By varying the simulations in MATLAB with different training algorithms, two models were trained for each measurand. The first model was trained using VLRBP while the second model was trained using CGB. For comparison with other types of neural networks such as recurrent, Elman networks, with one hidden layer consisting of ten neurons, were also developed for each measurand. As with the MLP networks, the VLRBP and the CGB algorithms were used to train the Elman networks. All the models were trained for a different number of epochs to let the errors converge to zero. The MSE performance function was used to measure each network's performance.

Tables 2 and 3 show the results obtained from all the developed models on non-training data for true position and circularity, respectively. Training multiple times generates different prediction results due to different initial conditions and sampling. Based on Tables 2 and 3, it can be concluded that both the feedforward and recurrent predictive models can provide accurate predictions for both measurands and the differences in the MSE values are very small especially for true position. Also, the models trained using CGB needed much less training epochs to achieve a low MSE value than the models trained using VLRBP.

Table 2. Performance of neural network models for true position.

	ANN Models	Epochs	Training algorithm	MSE (mm)
1	MLP-1	1000	VLRBP	7.37×10^{-7}
2	MLP-2	162	CGB	8.81×10^{-7}
3	Elman-1	1000	VLRBP	8.51×10^{-7}
4	Elman-2	70	CGB	6.95×10^{-7}

Table 3. Performance of neural network models for circularity.

	ANN Models	Epochs	Training algorithm	MSE (mm)
1	MLP-1	1000	VLRBP	4.46×10^{-6}
2	MLP-2	106	CGB	7.60×10^{-7}
3	Elman-1	1000	VLRBP	4.13×10^{-6}
4	Elman-2	118	CGB	4.56×10^{-6}

Tables 4 and 5 show the residual values, calculated by the difference between the Equator measured values and the model predictions, for true position and circularity, respectively. As can be seen from Tables 4 and 5, the residual values for true position are less than 1.5 μm for all the models while the residual values for circularity range in total from 0.2 to 5.6 μm for the first, third and fourth model and from 0.4 to 1.1 μm for the second model. It can be concluded that the proposed system provides a high degree of accuracy in predicting the end product quality and thus determining whether or not a product is within the allowable tolerances. However, in order to determine conformance or nonconformance to a tolerance, it is necessary to evaluate the uncertainty of predictions so that the risks involved in the product acceptance/rejection or re-engineering decision can be accurately assessed.

Table 4. Residuals for true position.

Parts	Model 1 (μm)	Model 2 (μm)	Model 3 (μm)	Model 4 (μm)
1	1.4	1.4	1.4	1.4
2	0.1	0.1	0.1	0.1
3	0.9	1.3	1.2	0.9
4	1.0	1.2	1.1	0.2
5	1.2	1.1	1.2	1.4
6	0.6	0.6	0.6	0.6
7	0.1	0.6	0.7	0.4
8	0.4	0.1	0.0	0.3

Table 5. Residuals for circularity.

Parts	Model 1 (μm)	Model 2 (μm)	Model 3 (μm)	Model 4 (μm)
1	0.9	0.9	0.9	1.2
2	0.9	1.1	0.6	0.2
3	0.9	1.1	0.9	1.1
4	0.7	0.4	0.7	0.4
5	1.0	1.0	1.0	0.8
6	0.3	0.8	0.9	0.9
7	1.1	0.7	1.0	0.9
8	5.5	0.7	5.3	5.6

5. Conclusions and future work

This paper has presented an intelligent metrology informatics system based on neural networks to transform the Multistage Manufacturing Process (MMP) data into knowledge of the process and part state and thus, supporting time-effective decision-making while minimising non-added value processes during part production. The MMP considered in this work included heat treatment, subtractive machining and post-process inspection. MLP and Elman networks were developed to predict the true position and circularity of the large bore of machined parts. The predicted results compared well with the experimental comparator measurements obtained from the Equator gauge. However, a limitation of this approach is the ability to only finding a single estimate for a feature characteristic without quantifying the associated uncertainty on the prediction. Therefore, future work will focus on developing learning algorithms that take into account the uncertainty in the metrology data.

Acknowledgements

The authors gratefully acknowledge funding for this research from the UK Engineering and Physical Sciences Research Council (EPSRC) under Grant Reference: EP/P006930/1.

References

[1] Schmitz TL, Ziegert JC, Canning JS, Zapata R. Case study: A comparison of error sources in high-speed milling. Prec Eng 2008;32:126-33.
[2] Papananias M, McLeay TE, Mahfouf M, Kadirkamanathan V. A Bayesian framework to estimate part quality and associated uncertainties in multistage manufacturing. Comput Ind 2019;105:35-47.
[3] Shi J. Stream of variation modeling and analysis for multistage manufacturing processes. CRC press; 2006.
[4] Karandikar J, McLeay TE, Turner S, Schmitz T. Tool wear monitoring using naïve Bayes classifiers. Int J Adv Manuf Technol 2015;77:1613-26.
[5] McLeay TE. Unsupervised monitoring of machining processes. PhD Thesis. University of Sheffield; 2016.
[6] Gandomi A, Haider M. Beyond the hype: Big data concepts, methods, and analytics. Int J Inf Manag 2015;35:137-44.
[7] He QP, Wang J. Statistical process monitoring as a big data analytics tool for smart manufacturing. J Proc Contr 2018;67:35-43.
[8] Kourti T. Application of latent variable methods to process control and multivariate statistical process control in industry. Int J Adapt Contr Sign Proc 2005;19:213-46.
[9] Ferrer A. Multivariate statistical process control based on principal component analysis (MSPC-PCA): Some reflections and a case study in an autobody assembly process. Qual Eng 2007;19:311-25.
[10] Chen Z, Lu S, Lam S. A hybrid system for SPC concurrent pattern recognition. Adv Eng Informat 2007;21:303-10.
[11] El-Midany TT, El-Baz MA, Abd-Elwahed MS. A proposed framework for control chart pattern recognition in multivariate process using artificial neural networks. Exp Sys Appl 2010;37:1035-42.
[12] Addeh A, Khormali A, Golilarz NA. Control chart pattern recognition using RBF neural network with new training algorithm and practical features. ISA Trans 2018;79:202-16.
[13] Özel T, Karpat Y. Predictive modeling of surface roughness and tool wear in hard turning using regression and neural networks. Int J Mach T Manuf 2005;45:467-79.
[14] Salgado DR, Alonso FJ, Cambero I, Marcelo A. In-process surface roughness prediction system using cutting vibrations in turning. Int J Adv Manuf Technol 2009;43:40-51.
[15] Huang PB. An intelligent neural-fuzzy model for an in-process surface roughness monitoring system in end milling operations. J Intell Manuf 2016;27:689-700.
[16] McCulloch WS, Pitts W. A logical calculus of the ideas immanent in nervous activity. Bull Math Biol 1943;5:115-33.
[17] Haykin S. Neural networks and learning machines. 3rd ed. New Jersey: Pearson; 2009.
[18] Manry MT, Chandrasekaran H, Hsieh CH. Signal processing using the multilayer perceptron. In: Hu YH, Hwang JN, editors. Handbook of neural network signal processing. CRC Press LLC; 2002.
[19] Forbes AB, Mengot A, Jonas K. Uncertainty associated with coordinate measurement in comparator mode. In: Laser Metrology and Machine Performance XI, LAMDAMAP. Huddersfield, UK; 2015.
[20] Papananias M, Fletcher S, Longstaff AP, Forbes AB. Uncertainty evaluation associated with versatile automated gauging influenced by process variations through design of experiments approach. Prec Eng 2017;49:440-55.
[21] Forbes AB, Papananias M, Longstaff AP, Fletcher S, Mengot A, Jonas K. Developments in automated flexible gauging and the uncertainty associated with comparative coordinate measurement. In: Euspen's 16th International Conference. Nottingham, UK; 2016.
[22] Papananias M, Fletcher S, Longstaff AP, Mengot A, Jonas K, Forbes AB. Modelling uncertainty associated with comparative coordinate measurement through analysis of variance techniques. In: Euspen's 17th International Conference. Hannover, Germany; 2017.
[23] Papananias M, Fletcher S, Longstaff AP, Mengot A, Jonas K, Forbes AB. Evaluation of automated flexible gauge performance using experimental designs. In: Laser Metrology and Machine Performance XII, LAMDAMAP. Wotton-under-Edge, UK; 2017.